

Atomistic analysis of the field-ion microscopy image of Fe₃Al

Chen Nan-xian

CCAST (World Lab), P.O. Box 8730, Beijing, 100080, China
and Beijing University of Science and Technology, Beijing, 100083, China

Ge Xi-jin, Zhang Wen-qing, and Zhu Feng-wu

Beijing University of Science and Technology, Beijing, 100083, China
(Received 24 February 1997; revised manuscript received 23 February 1998)

A unified lattice inversion method is applied to calculation of interatomic potentials and binding-energy differences between various kinds of surface atoms. Based on these calculated interatomic potentials, the field-ion microscopy images for Fe₃Al are discussed in detail in order to develop the general concept and the evaluation method of selective evaporation for binary ordered alloys. [S0163-1829(98)01022-4]

I. INTRODUCTION

The study of the field-ion microscopy (FIM) shows perfect ring structures in FIM images for pure metals. The size of concentric rings corresponds to the local curvature radius of the specimen's tip surface. Larger planar density of atoms corresponds to more prominent poles in the FIM images.^{1,2}

The clear ring structures also occur in the FIM images for binary ordered alloys.¹⁻⁶ However, there exists an additional phenomenon in experiment, which is called invisibility. That is, one of the species seems to have disappeared from FIM images for binary ordered alloys. For instance, Co atoms in L1₀ PtCo and Ni atoms in D1_α Ni₄Mo seem to be invisible in the corresponding FIM image.³⁻⁶ Apparently, the invisibility can be explained by selective evaporation assuming that the applied voltage can cause evaporation of surface atoms from the tip sample. According to previous works, atoms with lower sublimation energy value (in the pure metal state) are invisible since they seem to be evaporated easily, and the remaining atoms, which have higher sublimation energy (see Table I) in their pure metallic state, would preferably remain at the tip surface and construct the stable FIM image. We denote the sublimation energy for pure metal by E^s , then $E_{Co}^s < E_{Pt}^s$, and $E_{Ni}^s < E_{Mo}^s$. Therefore, the conception in previous works is apparently in good agreement with the experimental results.

II. PREVIOUS WORK ON FIM FOR Fe₃Al

Recently, the FIM image of Fe₃Al has been attracting attentions⁸⁻¹⁰ because of its potential applications.¹¹ Figure 1 shows the unit cell of a Fe₃Al superlattice. The DO₃ superlattice can be considered as eight B₂ structures stacked together to allow maximum distance between aluminum atoms. By comparing the sublimation energy values of pure metals Fe and Al, we can assert that Al should be the invisible species.⁸ However, in the experiment by Weng *et al.*,⁹ perfect rings, which correspond to a fcc structure, exist in the image of Fe₃Al. Given that the Al sublattice has the fcc structure, Weng *et al.* asserted that Fe is the invisible species in the image of Fe₃Al. Therefore, there is controversy on which kind of atoms is invisible. Note that the first argument

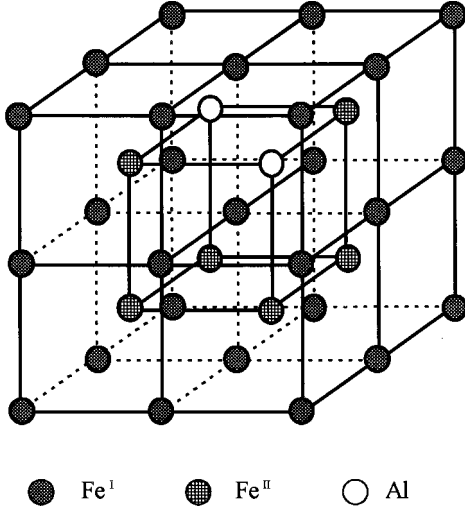
is based on two assumptions: (1) In a binary alloy one of the species is invisible, and the other is visible; (2) The atom with lower sublimation energy in its pure metallic state is invisible. Obviously, both assumptions are empirical rather than theoretical. Both have been used to successfully explain the FIM images of Ni₄Mo, Ni₃Al, and PtCo with the assertion that parameters such as sublimation energies for pure bulk metals are transferable to alloy's surfaces.

However, this explanation does not work for Fe₃Al. First, two types of Fe atoms exist in the DO₃ type of Fe₃Al, Fe^I and Fe^{II}. The Fe^I atoms at the "corners" form a simple cubic sublattice. The Fe^{II} atoms at the "centers" form a fcc sublattice that is identical with the Al atoms in Fe₃Al. Therefore, we have no reason to conclude from the experiment that the fcc-related rings in the FIM images for Fe₃Al are necessarily attributed to the Al atoms, and not to the Fe^{II} atoms, and likewise not to the Al and Fe^{II} atoms together. Second, since Al has a lower sublimation energy value compared to Fe, the Al atoms should be more easily evaporated than the Fe atoms. The visible atoms therefore should be Fe^{II} instead of Al.

In order to resolve the above controversy, one has to give up conventional premises. It is now necessary to consider the binding-energy difference between various kinds of surface atoms of Fe₃Al, which include Fe^I, Fe^{II}, and Al, and perhaps more. The evaluation of interatomic potentials Φ_{Al-Al} , Φ_{Fe-Fe} , and Φ_{Al-Fe} becomes the key issue. In the present work, a unified formula for inverse lattice problems¹² will be applied to obtain the pair potentials Φ_{Al-Al} , Φ_{Fe-Fe} , and Φ_{Al-Fe} based on *ab initio* calculated cohesive energy curves. The unified solution of the inverse lattice problems is presented in Sec. III with examples of the fcc, bcc, and DO₃ structures. Section IV shows the cohesive energy curves based on the *ab initio* calculation and the universal Rose equation¹³ for fcc Al, bcc Fe, and DO₃ Fe₃Al. In addition,

TABLE I. The sublimation energy values of various pure metals (Ref. 7).

Element	Pt	Co	Ni	Mo	Fe	Al
Sublimation energy (ev/atom)	5.84	4.39	4.44	6.82	4.28	3.39

FIG. 1. The unit cell of Fe₃Al (Ref. 9).

the converted pair potential curves $\Phi_{\text{Al-Al}}$, $\Phi_{\text{Fe-Fe}}$, and $\Phi_{\text{Al-Fe}}$ based on the unified lattice inversion formula are introduced. The above results will be used to evaluate the binding energies of various kinds of atoms on different surfaces of Fe₃Al. In true, the outcome of the evaluation will be compared to experimental data. The conclusion and discussion are in Sec. V.

III. THE INVERSE LATTICE PROBLEMS

The total energy of a Fe₃Al system containing N atoms includes three partial energies

$$U_{\text{Fe-Fe}}^{\text{Fe}_3\text{Al}}(x) = \frac{N}{4} \frac{1}{2} \sum_{(m,n,l) \neq (0,0,0)} \Phi_{\text{Fe-Fe}}(\sqrt{m^2+n^2+l^2}x) + \frac{N}{4} \frac{3}{2} \sum_{m,n,l} \Phi_{\text{Fe-Fe}}[\sqrt{(m-1/2)^2+(n-1/2)^2+l^2}x] \\ + \frac{N}{2} \frac{1}{2} \sum_{(m,n,l) \neq (0,0,0)} \Phi_{\text{Fe-Fe}}\left(\sqrt{m^2+n^2+l^2}\frac{x}{2}\right) + \frac{N}{4} \sum_{m,n,l} \Phi_{\text{Fe-Fe}}\left(\sqrt{(m-1/2)^2+(n-1/2)^2+(l-1/2)^2}\frac{x}{2}\right). \quad (3)$$

The last partial energy is composed of the interactions between the Al atoms and the Fe atoms, that is,

$$U_{\text{Fe-Al}}^{\text{Fe}_3\text{Al}}(x) = \frac{N}{4} \sum_{m,n,l} \Phi_{\text{Fe-Al}}\left(\sqrt{(m-1/2)^2+(n-1/2)^2+(l-1/2)^2}\frac{x}{2}\right) + \frac{N}{4} \sum_{m,n,l} \Phi_{\text{Fe-Al}}[\sqrt{(m-1/2)^2+(n-1/2)^2+(l-1/2)^2}x] \\ + \frac{3N}{4} \sum_{m,n,l} \phi_{\text{Fe-Al}}[\sqrt{m^2+n^2+(l-1/2)^2}x]. \quad (4)$$

The cohesive energy can be obtained by either *ab initio* calculation or experimental data combined with the application of universal Rose equation.¹³ In the next step, in order to determine the pairwise potentials $\Phi_{\text{Al-Al}}(x)$, $\Phi_{\text{Fe-Fe}}(x)$, and $\Phi_{\text{Fe-Al}}(x)$ based on the cohesive energy or the partial cohesive energy, we need to solve the inverse lattice problems.

$$U_{\text{tot}}^{\text{Fe}_3\text{Al}}(x) = U_{\text{Al-Al}}^{\text{Fe}_3\text{Al}}(x) + U_{\text{Fe-Fe}}^{\text{Fe}_3\text{Al}}(x) + U_{\text{Fe-Al}}^{\text{Fe}_3\text{Al}}(x), \quad (1)$$

where x is the lattice constant of Fe₃Al. The first term in the right-hand side corresponds to the interactions among Al atoms, the second one corresponds to the iron-iron interactions, and the last represents the contribution from the Fe-Al interactions.

A. Expression of inverse lattice problems

Now let us write down the expressions for $U_{\text{Al-Al}}^{\text{Fe}_3\text{Al}}(x)$, $U_{\text{Fe-Fe}}^{\text{Fe}_3\text{Al}}(x)$, and $U_{\text{Fe-Al}}^{\text{Fe}_3\text{Al}}(x)$ in terms of pairwise potentials. $U_{\text{Al-Al}}^{\text{Fe}_3\text{Al}}(x)$ is composed of the interatomic interactions between the Al atoms in the Al sublattice in Fe₃Al, that is

$$U_{\text{Al-Al}}^{\text{Fe}_3\text{Al}}(x) = \frac{N}{4} \frac{1}{2} \sum_{(m,n,l) \neq (0,0,0)} \Phi_{\text{Al-Al}}(\sqrt{m^2+n^2+l^2}x) \\ + \frac{N}{4} \frac{3}{2} \sum_{m,n,l} \Phi_{\text{Al-Al}} \\ \times [\sqrt{(m-1/2)^2+(n-1/2)^2+l^2}x], \quad (2)$$

and $U_{\text{Fe-Fe}}^{\text{Fe}_3\text{Al}}(x)$ is composed of the interatomic potentials between the Fe atoms, including Fe^I and Fe^{II}. This can be expressed as

B. Carlsson-Gelatt-Ehrenreich technique (Ref. 16)

For most applications the pair potential approximation is considered to have spherical symmetry. And in various situations either the Lennard-Jones form is used for Van der Waals solids,¹⁴ or the different modified Morse-type potentials are used for metals¹⁵ extensively. The simplicity of pair

potentials has made it possible to study the mechanical and defect properties of metals, on the other hand, to study the phase diagram of binary alloys, and the para- to antiferromagnetic transition problem. Most previous works only treat the nearest-neighbor interactions. Carlsson *et al.*¹⁶ used *ab initio* band-structure calculation to obtain a pair potential with long-range interactions.

Band-structure calculation can produce the total energy, $E_{\text{tot}}(r)$, as a function of lattice constant r . In general, the cohesive energy $E(r) = E_{\text{tot}}(r) - E_{\text{tot}}(\infty)$ for each atom in a three-dimensional crystal lattice can be expressed as a sum of interatomic pair potentials $\Phi(x)$ such that

$$E(r) = \frac{1}{2} \sum_{\mathbf{R} \neq 0} \Phi(\mathbf{R}), \quad (5)$$

where r is the lattice constant, \mathbf{R} is the lattice vector. For concrete deduction, let us assume that each term at a fixed value of $S_p r$ occurs with a given weight W_p in the sum (5). These pairs of values $\{S_p, W_p\}$ are specific to a given lattice structure, and can be easily generalized for different lattices by computer. Thus we may rewrite Eq. (5) as

$$E(r) = \sum_{p=1}^{\infty} W_p \Phi(S_p r). \quad (6)$$

In fact, denoting that $E(x) = U(x)/N$, all the Eqs. (2)–(4) will take the same form as Eq. (6). Now define an operator \mathfrak{R} such that

$$E(r) = \mathfrak{R} \Phi(r) = \left[\sum_{p=1}^{\infty} \mathfrak{R}_p \right] \Phi(r), \quad (7)$$

where the operator \mathfrak{R}_p is defined by

$$\mathfrak{R}_p f(r) = W_p f(S_p r), \quad (8)$$

in which $f(r)$ is an arbitrary function. The formal inversion is then

$$\Phi(r) = \mathfrak{R}^{-1} E(r). \quad (9)$$

Carlsson *et al.* define \mathfrak{R}^{-1} as

$$\mathfrak{R}^{-1} = \left(1 + \mathfrak{R}_1^{-1} \sum_{p=2}^{\infty} \mathfrak{R}_p \right)^{-1} \mathfrak{R}_1^{-1}, \quad (10)$$

so that it is given as

$$\begin{aligned} \Phi(r) = & \left(\frac{1}{W_1} \right) E \left(\frac{r}{S_1} \right) - \sum_{p=2}^{\infty} \left(\frac{W_p}{W_1^2} \right) E \left(\frac{S_p r}{S_1} \right) \\ & + \sum_{p=2}^{\infty} \sum_{q=2}^{\infty} \left(\frac{W_p W_q}{W_1^3} \right) E \left(\frac{S_p S_q r}{S_1^3} \right) - \dots \end{aligned} \quad (11)$$

The right-hand side of Eq. (11) consists of infinite sums, each of them has infinite terms. The convergence of this series is slow, and is analyzed with difficulty. Thus we shall illustrate an alternative method based on a generalized Möbius transform as follows.

C. Generalized Chen-Möbius inversion formula (Ref. 12)

For convenience, we replace the lattice constant r by the nearest-neighbor distance x , correspondingly, $\{S_p\}$ by $\{b_0(n)\}$, and $\{W_p\}$ by $\{r_0(n)\}$, such that

$$E(x) = \frac{1}{2} \sum_{n=1}^{\infty} r_0(n) \Phi(b_0(n)x), \quad (12)$$

where $b_0(n)$ in a monotonically increasing series represents the distance between the origin on which the reference atom is located and the n th set of lattice points, $r_0(n)$ is the number of the n th set of lattice points. For example, $b_0(1) = 1$ corresponds to the nearest-neighbor distance. The inverse lattice problem is to determine $\Phi(x)$ from the fitting curve of $E(x)$, which can be obtained from the *ab initio* calculation. The trick here is to extend the series $\{b_0(n)\}$ to $\{b(n)\}$ to achieve multiplicative closedness. Thus, for any m and n , there exist k such that

$$b(k) = b(m)b(n). \quad (13)$$

In other words, $\{b_0(n)\}$ can always be replaced by a multiplicative semigroup $\{b(n)\}$. Therefore, Eq. (12) is equivalent to the following:

$$E(x) = \frac{1}{2} \sum_{n=1}^{\infty} r(n) \Phi(b(n)x), \quad (14)$$

in which

$$r(n) = \begin{cases} r_0(b_0^{-1}[b(n)]), & \text{if } b(n) \in \{b_0(n)\}, \\ 0, & \text{if } b(n) \notin \{b_0(n)\}. \end{cases} \quad (15)$$

The lattice point shell is called virtual when $r(n) = 0$.

Then the solution to Eq. (14) is given by

$$\Phi(x) = 2 \sum_{n=1}^{\infty} I(n) E(b(n)x), \quad (16)$$

in which the inversion coefficient or the generalized Möbius function $I(n)$ is given by

$$\sum_{b(n)|b(k)} I(n) r \left(b^{-1} \left[\frac{b(k)}{b(n)} \right] \right) = \delta_{k1}. \quad (17)$$

This indicates that $I(n)$ and $r(n)$ are the modified Dirichlet inverse of each other, which is a generalization of common Dirichlet inverse in number theory. The following proves that Eq. (16) is the solution to Eq. (14), as well as to Eq. (12):

$$\begin{aligned} & 2 \sum_{n=1}^{\infty} I(n) E(b(n)x) \\ &= \sum_{k=1}^{\infty} \left\{ \sum_{b(n)|b(k)} I(n) r \left(b^{-1} \left[\frac{b(k)}{b(n)} \right] \right) \right\} \Phi(b(k)x) \\ &= \sum_{k=1}^{\infty} \delta_{k1} \Phi(b(k)x) = \Phi(b(1)x) = \Phi(x). \end{aligned}$$

In the case of $[b(n)]^2$ not being integers, the least common multiple of all the denominators can be used in the recursive

procedure. The solution (16) with Eq. (17) can be applied to any lattice structure of interest in condensed-matter physics or statistical physics. Several examples relevant to this work are provided as follows.

From a mathematical point of view, the general expression $r_0(n)$ of the number of the crystallographic lattice points on a spherical surface is unsolved, but this can be obtained regirously by a very simple computer program up to the shell as large as required. After this step, a generalized Dirichlet inverse can be introduced. And it is shown that once the technique in number theory is applied, the problem can be solved in an unexpectedly concise manner.

D. Inversion formula for a fcc structure (Ref. 12)

The inverse problem can be expressed as

$$E(x) = \frac{1}{2} \sum_{\{i,j,k\} \neq 0} \Phi[\sqrt{2(i^2+j^2+k^2)}x] \\ + \frac{3}{2} \sum_{i,j,k} \Phi\left\{ \sqrt{2\left[\left(i-\frac{1}{2}\right)^2 + \left(j-\frac{1}{2}\right)^2 + k^2\right]}x \right\} \\ = \sum_{n=1}^{\infty} r(n)\Phi(b_0(n)x). \quad (18)$$

The corresponding solution is

$$\Phi(x) = \frac{1}{12}E(x) - \frac{1}{24}E(\sqrt{2}x) - \frac{1}{6}E(\sqrt{3}x) - \frac{1}{16}E(2x) \\ - \frac{1}{6}E(\sqrt{5}x) + \dots \quad (19)$$

In the present work, we use this fcc lattice inversion formula to obtain the pairwise potential $\Phi_{\text{Al-Al}}(x)$ based on the cohesive energy curve for the fcc metal Al.

E. Inversion formula for a bcc structure (Ref. 12)

For obtaining the pair potential $\Phi_{\text{Fe-Fe}}(x)$ from the cohesive energy curve for iron with bcc structure, we need to solve the equation of the inversion problem of a bcc lattice, which can be expressed as

$$E(x) = \frac{1}{2} \sum_{n=1}^{\infty} \Phi(b(n)x) \\ = \frac{1}{2} \sum_{(l,m,n) \neq (0,0,0)} \left[\Phi\left(\sqrt{\frac{4}{3}\{l^2+m^2+n^2\}}x\right) \right. \\ \left. + \Phi\left(\sqrt{\frac{4}{3}\left[\left(l-\frac{1}{2}\right)^2 + \left(m-\frac{1}{2}\right)^2 + \left(n-\frac{1}{2}\right)^2\right]}x\right) \right]. \quad (20)$$

The corresponding solution is given as follows:

$$\Phi(x) = \frac{1}{4}E(x) - \frac{3}{16}E\left(\sqrt{\frac{4}{3}}x\right) + \frac{9}{64}E\left(\frac{4}{3}x\right) \\ - \frac{27}{256}E\left(\sqrt{\frac{64}{27}}x\right) + \dots \quad (21)$$

F. Inversion formula for a DO₃ structure

The inverse lattice problem for a DO₃ structure or the relation between the total energy and partial energies can be expressed as

$$E_{\text{Al-Fe}}(x) = \frac{1}{N} [U_{\text{total}}^{\text{Fe}_3\text{Al}}(x) - U_{\text{Al-Al}}^{\text{Fe}_3\text{Al}}(x) - U_{\text{Fe-Fe}}^{\text{Fe}_3\text{Al}}(x)]. \quad (22)$$

The relation between the partially cohesive energy $E_{\text{Al-Fe}}(x)$ and pairwise potential $\Phi_{\text{Al-Fe}}(x)$ is

$$E_{\text{Al-Fe}}(x) = 8\Phi_{\text{Al-Fe}}(x) + 6\Phi_{\text{Al-Fe}}\left(\sqrt{\frac{4}{3}}x\right) \\ + 24\Phi_{\text{Al-Fe}}\left(\sqrt{\frac{11}{3}}x\right) + 8\Phi_{\text{Al-Fe}}\left(\sqrt{\frac{19}{3}}x\right) \\ + 24\Phi_{\text{Al-Fe}}\left(\sqrt{\frac{20}{3}}x\right) + 24\Phi_{\text{Al-Fe}}(3x) + \dots \quad (23)$$

The corresponding solution is given as

$$\Phi_{\text{Al-Fe}}(x) = \frac{1}{8}E_{\text{Al-Fe}}(x) - \frac{3}{32}E_{\text{Al-Fe}}\left(\sqrt{\frac{4}{3}}x\right) \\ + \frac{9}{128}E_{\text{Al-Fe}}\left(\frac{4}{3}x\right) - \frac{27}{512}E_{\text{Al-Fe}}\left(\frac{8}{3\sqrt{3}}x\right) \\ + \frac{81}{2048}E_{\text{Al-Fe}}\left(\frac{16}{9}x\right) + \dots \quad (24)$$

IV. CALCULATION AND EXPLANATION OF FIM IMAGE OF Fe₃Al

A. Energy analysis

Let us consider a system of Fe₃Al, which consists of N atoms. The total energy of this system can be expressed as the sum of three parts:

$$U_{\text{tot}}^{\text{Fe}_3\text{Al}} = U_{\text{Fe-Fe}} + U_{\text{Al-Al}} + U_{\text{Al-Fe}}.$$

Step 1: To evaluate $U_{\text{Fe-Fe}}^{\text{Fe}_3\text{Al}}(x)$ based on $\Phi_{\text{Fe-Fe}}(x)$. The latter can be converted from $E_{\text{coh}}^{\text{bcc Fe}}(x)$ in terms of the unified lattice inversion formula for a body-centered cubic structure;

Step 2: To evaluate $U_{\text{Al-Al}}^{\text{Fe}_3\text{Al}}(x)$ based on $\Phi_{\text{Al-Al}}(x)$. The latter can be converted from $E_{\text{coh}}^{\text{fcc Al}}(x)$ in terms of the unified lattice inversion formula for a face-centered-cubic structure;

Step 3: To evaluate $U_{\text{Al-Fe}}$ from $U_{\text{Fe}_3\text{Al}}^{\text{tot}}(x) - U_{\text{Fe-Fe}}(x) - U_{\text{Al-Al}}$;

Step 4: To convert $U_{\text{Al-Fe}}$ into $\Phi_{\text{Al-Fe}}$ based on the unified lattice inversion formula for a shifted simple cubic structure;

Step 5: To evaluate the cohesive energies $E_{\text{Al}}^{\text{sur}}$ and $E_{\text{Fe}}^{\text{sur}}$ of surface atoms for surfaces with different indices.

B. The cohesive energy curves of Al, Fe, and Fe₃Al

A few parameters are needed to establish the cohesive energy curves based on Rose's universal equation of states as

TABLE II. The *ab initio* calculated parameters for related metals.

Metal	Structure	Sublimation energy (eV)	Lattice constant a_0 (Å)	Bulk modulus (10^{12} dyn/cm ²)
Al	fcc	3.39 (exp)	4.05 (exp)	0.722 (exp)
Fe	bcc	4.87 (exp)	2.87 (exp)	1.683 (exp)
Fe ₃ Al	DO ₃	4.40(cal)	5.57(cal)	2.29 (exp)
		4.22(exp)	5.792(exp)	

$$E_0(a') = E_0(1 + a')e^{-a'}, \quad (25)$$

where $a' = \beta(x - x_0)$, E_0 is the sublimation energy, x_0 is the equilibrium nearest-neighbor distance, and $\beta = (9B\Omega_0/x_0^2E_0)^{1/2}$, in which B is the bulk modulus and Ω_0 is the equilibrium atomic volume. Therefore, for each cohesive energy curve three parameters x_0 , E_0 , and B are required. For most pure metals, the experimental data can be found easily, which are taken for the present work. For the ordered alloys, part of experimental data are hardly obtained, which will be calculated from *ab initio* linear-argumented plane-wave calculation. For example, the bulk modulus of Fe₃Al is difficult to measure due to its brittleness, thus the calculated data is taken. These equilibrium parameters are listed in Table II.

C. The interatomic potentials $\Phi_{\text{Al-Al}}$, $\Phi_{\text{Fe-Fe}}$, and $\Phi_{\text{Fe-Al}}$

Now the lattice inversion formulas are used in order to obtain the interatomic potentials $\Phi_{\text{Al-Al}}$, $\Phi_{\text{Fe-Fe}}$, and $\Phi_{\text{Fe-Al}}$, the results are shown in Figs. 2 and 3.

D. The calculation of evaporating energies

Based on the interatomic potentials $\Phi_{\text{Al-Al}}$, $\Phi_{\text{Fe-Fe}}$, and $\Phi_{\text{Fe-Al}}$, we can evaluate the binding energies or evaporating energies of various surface atoms of Fe₃Al (see Table III). The calculated evaporating energies are listed in eV. Only surfaces with indices (100), (110) or (111) have two or three kinds of Fe atoms. For different surfaces the invisible atoms

are different. For instance, Fe^I and Fe^{II} are invisible on surfaces (100) and (111), and Fe^I on surface (110). Therefore, Fe^I atoms are always invisible and Fe^{II} are sometimes invisible. The condition is that the applied voltage arrives at a certain value such that evaporation occurs, and the FIM images are attributed to the remaining atoms. The probabilities for competitive evaporation of different kinds of surface atoms can be evaluated by the Boltzmann distribution, which is temperature dependent. The smaller the probability for evaporation, the longer the duration of the stationary FIM image obtained in experiment. Note that there are two kinds of surfaces that consist of the Fe^I atoms with indential index (111) as shown in Fig. 4. This is why the binding energy of surface atoms Fe^I takes two values as in Table III.

V. CONCLUSION AND DISCUSSION

As long as selective evaporation dominates, the experimental results agree well with the atomistic simulation of the FIM image formation based on the approximately universal Rose cohesive energy curve with *ab initio* calculated or experimental parameters and the universal lattice inversion method within the pair-potential approximation. In fact, the present method has been proven to work well not only for Fe₃Al,^{9,10} but also for Ni₄Mo, PtCo, PtCo₃, Ni₃Fe, and Ni₃Al. According to the conventional selective evaporation rule, we will obtain the wrong conclusion for most of these ordered alloys.¹⁷

According to convention, both selective ionization (elec-

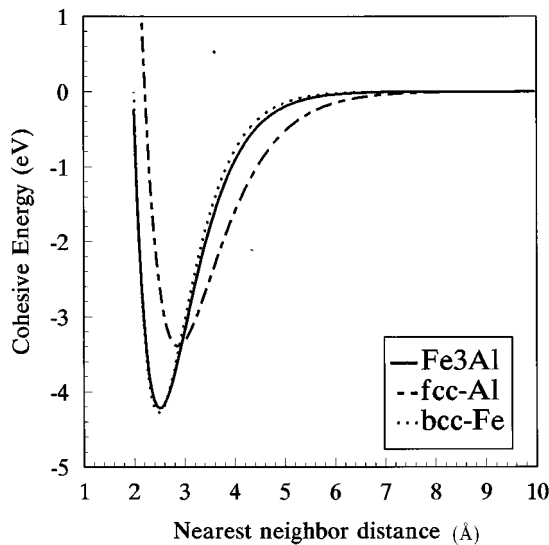


FIG. 2. The binding-energy curves for fcc Al, bcc Fe, and DO₃ Fe₃Al based on *ab initio* calculation and Rose formula.

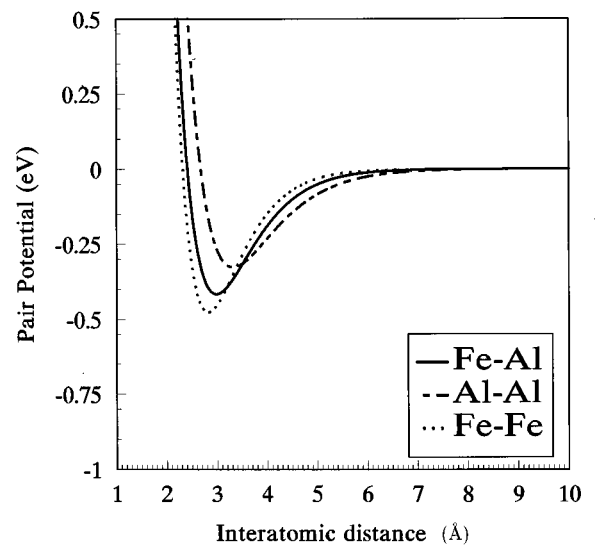


FIG. 3. The pair potentials $\Phi_{\text{Al-Al}}$, $\Phi_{\text{Fe-Fe}}$, and $\Phi_{\text{Al-Fe}}$ converted from binding-energy curves $E_{\text{Al-Al}}$, $E_{\text{Fe-Fe}}$, and $E_{\text{Al-Fe}}$.

TABLE III. Binding energy of various surface atoms of Fe₃Al.

Binding energy (eV)	(100)	(110)	(111)
Fe ^I	5.319	5.381	4.317/4.648
Fe ^{II}	5.322	5.618	4.595
Al	5.822	5.723	5.145

tronic charge transfer) and selective evaporation are possible methods to explain the selective invisibility for different kinds of atoms in the stable FIM images of a binary ordered alloy. When the applied voltage is not high enough to cause selective evaporation, the electron transfer between different kinds of atoms will dominate the FIM images. Weng *et al.*⁹ compare the work function values of component atoms of Fe₃Al in its pure metallic state. In fact, the work function is a characteristic of metal such as iron or aluminum, not that for atoms. In our case, the experiment was done in the condition that the applied voltage was high enough to cause selective evaporation at first, then we decreased the voltage for a stable FIM image. If we use the conventional rule of selective evaporation, the Al atoms would evaporate easily and it would be invisible, and this is contrary to experiment (see Table I).

From a theoretical point of view, the many-body effect should be considered for a general situation. Also, the surface relaxation might be important. These will be for further study.

Finally we like to discuss the uncertainties in the approximations we used. First, the pair potential model is only a popular and very simple approximation of interatomic approximation, especially for the surface atoms. Second, even the inversion procedure is suitable for any kind of cohesive energy curves, the curve can be obtained in different ways:

- (a) direct *ab initio* calculation,
- (b) Rose approximation based on *ab initio* calculated E_0, a_0 , and B,

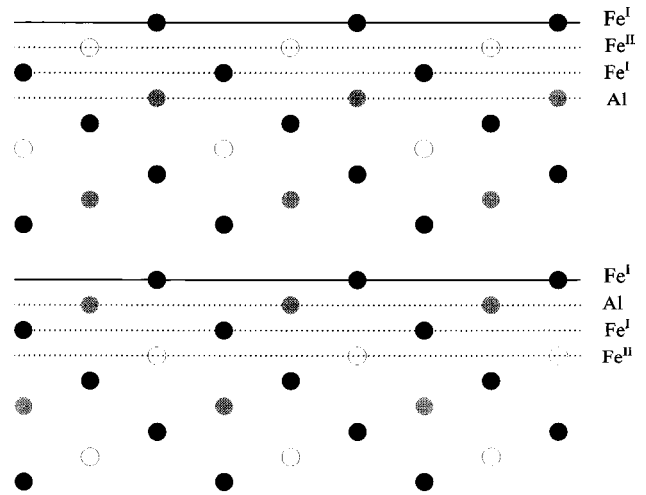


FIG. 4. When (111) surface is occupied by Fe^I atoms, there are two different cases: the next layer consists of (1) only Al atoms, (2) only Fe^{II} atoms.

- (c) Morse approximation based on *ab initio* calculated E_0, a_0 , and B,
- (d) Rose approximation based on experimental E_0, a_0 , and B,
- (e) Morse approximation based on experimental E_0, a_0 , and B,
- (f) others.

ACKNOWLEDGMENTS

The authors would like to express their thanks to Professor Z. G. Liu, Q. J. Gao, and Dr. J. Weng for helpful discussions and encouragement. This work was supported partly by National Foundation of Natural Science in China, and partly by National Advanced Materials Committee of China.

¹E.W. Müller and T.T. Tsong, *Field Ion Microscopy, Principles and Applications* (Elsevier, New York, 1969).

²M.K. Miller and C.D.W. Smith, *Atom Probe Microanalysis* (Materials Research Society, Pittsburgh, PA, 1989).

³H.N. Southworth and B. Ralph, *Philos. Mag.* **14**, 383 (1966).

⁴T.T. Tsong and E.W. Müller, *J. Appl. Phys.* **38**, 545 (1967).

⁵M. Yamamoto, M. Futamoto, S. Nenno, and S. Nakamura, *J. Phys. Soc. Jpn.* **36**, 1330 (1974).

⁶T.T. Tsong, S.V. Krishawamy, S.B. Maclane, and E.W. Müller, *Appl. Phys. Lett.* **23**, 1 (1974).

⁷C. Kittel, *Introduction to Solid State Physics*, 6th ed. (Wiley, New York, 1986).

⁸H.J. Krause, J.E. Wittig, and G. Frommeyer, *Z. Metallkd.* **78**, 576 (1987).

⁹J. Weng, F.W. Zhu, and J.M. Xiao, *Z. Metallkd.* **85**, 432 (1994).

¹⁰Z.G. Liu, G. Frommeyer, M. Kreuss, J. Wesemann, and N. Wanderka (unpublished).

¹¹C.G. McKamey, J.H. DeVan, P.F. Tortorelli, and V.K. Sikka, *J. Mater. Res.* **6**, 1779 (1991).

¹²N.X. Chen, Z.D. Chen, and Y.C. Wei, *Phys. Rev. E* **55**, R5 (1997).

¹³J.M. Rose, J.R. Smith, F. Guinea, and J. Ferrante, *Phys. Rev. B* **29**, 2963 (1984).

¹⁴F.F. Abraham, *J. Vac. Sci. Technol. B* **2**, 534 (1984).

¹⁵R.A. Johnson, *Phys. Rev. B* **37**, 3924 (1988); **37**, 6121 (1988).

¹⁶A.E. Carlsson, C.D. Gelatt, and H. Ehrenreich, *Philos. Mag. A* **41**, 241 (1980).

¹⁷N.X. Chen and X.J. Ge (unpublished).